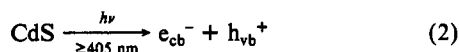


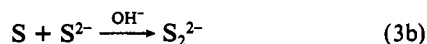
SO_3^{2-} to $\text{S}_2\text{O}_3^{2-}$ and CN^- to SCN^- are very similar, if not identical.

Discussion

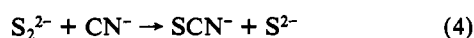
The presently available results suggest the following pathway for the complete photocatalyzed transformation of cyanide to the less toxic form thiocyanate. The CdS particles absorb visible light to produce electron/hole pairs according to reaction 2. The



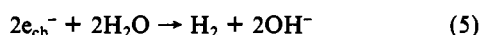
valence band holes react with S^{2-} to give sulfur, which dissolves in alkaline solution as polysulfides S_n^{2-} (eq 3) containing sulfane



sulfur. Polysulfide ions are known to react with CN^- , a powerful thiophile,¹⁸ to form SCN^- (eq 4)¹⁹ in a manner parallel to the one



observed in the transformation of SO_3^{2-} to $\text{S}_2\text{O}_3^{2-}$.²⁰ No conversion occurs between S^{2-} and CN^- in the absence of CdS/0.2 wt % Rh and/or light, confirming that h_{vb}^+ is necessary to oxidize S^{2-} and thereby mediate the CN^- to SCN^- transformation. The conduction band electrons, e_{cb}^- , reduce water to hydrogen (eq 5)



and are involved in the electron/hole pair recombination. The presence of a redox catalyst (RuO₂ or Rh) on CdS is necessary to ensure SCN^- formation and prevent photocorrosion, a result that might be due to photocomplexation of Cd²⁺(lattice) by CN^- ions; the mechanism is not yet clear.²¹

Insofar as the reactivity of the CdS/0.2 wt % Rh catalyst in the presence and absence of O₂ is concerned, the results confirm

some of our earlier findings in the $\text{S}_2\text{O}_3^{2-}$ synthesis.¹⁴ However, in the present instance, oxygen does not alter the 1:1 distribution of the products ($\text{H}_2\text{:SCN}^-$). Experiments to elucidate the difference(s) between the behavior of SO_3^{2-} and CN^- are under investigation.²²

The quantum efficiency for the CN^-/SCN^- conversion is $\geq 0.25 \pm 0.05$ at 436 nm (see ref 14 for details). It is important to note that this value is a lower limit and is based on the total number of incident photons that reach the sample. No doubt, a more efficient CdS powder^{14,23} and optimization of the photoreactor^{10a} may lead to improvements in the quantum efficiency of the process.

Conclusions

Disposal of CN^- ions by photochemical methods with the participation of the Rh-loaded CdS catalyst (or an equivalent one) opens up a potential practical alternative to the present methods in the transformation of CN^- to SCN^- that employs inexpensive materials and abundant sunlight.^{10a} The conversion is efficient even in the presence of air and, more important, even at very high cyanide concentrations. As an added advantage, hydrogen is a useful byproduct. Moreover, where both sulfide and cyanide are available, the conversion process(es) can dispose of two toxic materials.^{2,9,24}

Acknowledgment. This work has benefited from support by the National Sciences and Engineering Research Council of Canada and by the Consiglio Nazionale delle Ricerche, Rome, through its Progetto Finalizzato, "Chimica Fine e Secondaria", to whom we are grateful. We also thank NATO for support (Grant No. 843/84) of the exchange between our respective laboratories.

Registry No. CN^- , 57-12-5; SCN^- , 302-04-5; CdS, 1306-23-6; Rh, 7440-16-6; Na₂S, 1313-82-2; NaCN, 143-33-9.

- (18) Westley, J. In *Cyanide in Biology*; Vennesland, B., Conn, E. E., Knowles, C. J., Westley, J., Wissing, F., Eds.; Academic: New York, 1981; p 61.
- (19) Schulek, E. Z. *Anal. Chem.* **1925**, *65*, 352.
- (20) Wober, A. *Angew. Chem.* **1921**, *34*, 73.
- (21) Experiments on the photostability of CdS/Rh vs. that of naked CdS in alkaline solutions of Na₂S and NaCN are under way. We are intrigued by the possibility of a sulfur/cyanide exchange in the CdS lattice under visible light irradiation; this appears to be a determining factor in the efficiency of the conversion process.
- (22) The reaction between S^{2-} and O₂ to give S and O₂²⁻ is under investigation (D. Meisel, personal communication) and ought to be compared to $\text{S}^{2-} + \text{SO}_2^{2-} \rightarrow$ (intermediates) and $\text{O}_2^{2-} + \text{CN}^- \rightarrow$ (intermediates) in order to confirm or deny the validity of our hypothesis.
- (23) Serpone, N.; Borgarello, E.; Barbeni, M.; Pelizzetti, E. *Inorg. Chim. Acta* **1984**, *90*, 191.
- (24) (a) *Hydrogen Sulfide in the Atmospheric Environment: Scientific Criteria for Assessing its Effects on Environmental Quality*; Pub. No. NRCC 18467; Associate Committee on Scientific Criteria for Environmental Quality, National Research Council of Canada: Ottawa, Canada, 1981. (b) *Hydrogen Sulfide*; Subcommittee on Hydrogen Sulfide, Committee on Medical and Biologic Effects of Environmental Pollutants, Division of Medical Sciences, Assembly of Life Sciences, National Research Council; University Park Press: Baltimore, MD, 1979.

Contribution from the Department of Chemistry, Northwestern University, Evanston, Illinois 60201

Electrochemistry and Spectroscopy of $\text{Fe}(\text{phen})_2(\text{CN})_2$, $\text{Cp}_4\text{Fe}_4(\text{CO})_4$, and $\text{CpFe}(\text{CO})_2\text{CN}$ in an Acidic Molten Salt

Carrie Woodcock and Duward F. Shriver*

Received November 26, 1985

Three basic organometallic compounds, $\text{Fe}(\text{phen})_2(\text{CN})_2$ (**1**), $\text{Cp}_4\text{Fe}_4(\text{CO})_4$ (**2**), and $\text{CpFe}(\text{CO})_2\text{CN}$ (**3**), have been studied in the AlCl_3/n -butylpyridinium chloride (BPC) molten salt system. IR and UV-vis spectroscopies show that the ligands of all three complexes interact with Lewis acids contained in the melts, i.e. FeCN-Al and $\text{Fe}_3\text{CO-Al}$. Melts with molar ratios of AlCl_3 to BPC less than 1, previously referred to as "basic", behave as weak Lewis acids relative to compound **1**, and melts with ratios greater than 1 behave as strong Lewis acids toward all three compounds. A comparison of spectral shifts for these compounds in the various melts with shifts previously reported for isolated Lewis acid adducts of the same compounds provides insight into the relative electron pair acceptor ability of the various melts. Cyclic voltammetry of **1** in the molten salts demonstrates a very large shift in the oxidation potential whereas the oxidation potential of **2** is unchanged. We infer that the HOMO of **1** is strongly perturbed by interaction with the Lewis acids in the molten salt whereas for **2** the HOMO is unaffected. This interpretation is consonant with simple molecular orbital calculations.

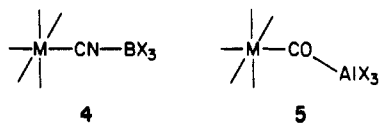
Introduction

Lewis acids can dramatically influence the electronic structure of metal complexes having basic CN and CO ligands. For example, Lewis acid adducts of these complexes often exhibit altered

electronic spectra,^{1,2} electrochemistry,¹ and reactivity.³⁻⁵ In all of these cases, the Lewis acid appears to perturb the metal complex

(1) Shriver, D. F.; Posner, J. J. *Am. Chem. Soc.* **1966**, *88*, 1672.

by the formation of ligand-bridged adducts such as 4 and 5. The



recent development of an acidic ambient-temperature molten salt system⁶ captured our attention as a promising medium for the electrochemical study of complexes containing ambidentate ligands. An attractive feature of this molten salt is that the acidity can be altered by varying the ratio, M_R , of the two components, $AlCl_3$ and *n*-butylpyridinium chloride.⁶

In the present investigation, we have utilized this molten salt for an electrochemical and spectroscopic study of three compounds, $Fe(phen)_2(CN)_2$,^{7,8} $Cp_4Fe_4(CO)_4$,⁹ and $CpFe(CO)_2(CN)$ ¹⁰ (phen = 1,10-phenanthroline, Cp = cyclopentadienyl), known to form simple ligand-bridged adducts with Lewis acids.^{1,10,11} Evidence for adduct formation has been reported for amines¹² and quinones¹³ dissolved in the highly acidic melts, and the electrochemistry of some metal carbonyl complexes and metallocenes in this molten salt has been investigated.^{14,15} The research described here focuses on inorganic complexes containing ligands that are highly sensitive to the Lewis acidity of their environment, thereby providing convenient spectroscopic probes into the donor-acceptor properties of these molten salts.

Experimental Section

Materials. $Fe(phen)_2(CN)_2$,^{7b} $Cp_4Fe_4(CO)_4$,⁹ and $CpFe(CO)_2(CN)$ ¹⁰ were prepared by the published procedures. Methylene chloride and chloroform were dried by standard methods.¹⁶ Aluminum trichloride and *n*-butylpyridinium chloride were prepared and purified according to established procedures.⁶ The melts were prepared in a drybox under continuous N_2 purge by slowly adding the ground $AlCl_3$ to the BPC contained in a beaker equipped with a magnetic stir bar. The rate of addition was such that the melt temperature never exceeded 60 °C. Occasionally, the more acidic melts were slightly yellow. This apparently had no effect on the spectroscopic or electrochemical properties of the compounds under study.

Spectroscopic Measurements. Electronic spectra were recorded on a Perkin-Elmer Model 330 spectrophotometer. Molten salt samples were prepared in a drybox and added to a vacuum-tight 1-mm pathlength cell.¹⁷

Infrared spectra were recorded on a Nicolet 7199 Fourier transform infrared spectrophotometer. Samples were prepared in the drybox by using CaF_2 cell windows with Teflon spacers (usually 0.10 mm). Care was taken to minimize contact of the molten salts with the stainless-steel cell holder. Tightly fitting rubber septa were used to exclude air from the cells. In each case, a background spectrum was recorded on the pure melt, and then the cell was returned to the drybox and flushed with the same melt containing the compound of interest. The sample spectrum was recorded, and a point by point subtraction routine was used to obtain the final spectrum.

Electrochemical Measurements. Electrochemistry was performed with a Princeton Applied Research Model 373 potentiostat/galvanostat

equipped with a in-house-built digital controller. The high-impedance voltage amplifier (PAR Model 178) was mounted external to the potentiostat to minimize noise pickup.

Cyclic voltammograms were performed in a cylindrical cell $3/4$ in. in diameter and 7 in. tall. For the molten salt studies, the working electrode was a glassy-carbon disk (0.084 cm² area) mounted in a Kel-F body (BAS) and the counter electrode was made from aluminum wire (1.0 mm diameter, Aldrich Gold Label) coiled once around the base of the working electrode. The reference electrode was a straight Al wire isolated from the other electrodes by a 5-mm gas dispersion tube (4–8- μ m pore diameter; Ace Glass Inc.) containing pure melt. The electrolyte level in the reference compartment was maintained slightly higher than that of the bulk solution. The three electrodes were attached via gold connectors to tungsten wires sealed through the cap of the cell. The cap was attached to the body of the cell by a 15-mm O-ring joint. Both the cell and cap were fitted with Teflon valves for Schlenk line manipulations. The cell was immersed in an oil bath maintained at 40 °C (± 2 °C) by a Variac. Voltammograms in methylene chloride were recorded at room temperature. In this case, the counter electrode was fashioned from 0.02-in. diameter platinum wire and the reference electrode was a silver wire dipping directly into the solution. All voltammograms were standardized to a small amount of ferrocene added after recording the voltammogram of interest. In all cases, a volume of only 3 mL was required for the cyclic voltammograms. The voltammograms were recorded on a Houston Model 205 XY recorder.

Bulk electrolyses were performed in a two-compartment cell containing 15-mm O-ring joints. The compartments were separated by a 10-mm frit (10–20- μ m pore diameter). The working electrode was constructed from reticulated vitreous carbon (RVC) (E.R.G., Inc.) and the counter electrode was a coil of aluminum wire. The reference electrode was identical with that used in the voltammetry experiments and was located as close as possible to the RVC electrode. The solution was stirred with a Teflon-coated magnetic stir bar, and the total charge passed was measured with a coulometer.

Diffusion coefficients were measured using chronoamperometry. The current decay as a function of time was monitored on the XY recorder and plots of i_t vs. $t^{-1/2}$ yielded straight lines for 0.5 s < t < 3.5 s. Diffusion coefficients were calculated from the Cottrell equation¹⁸

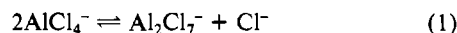
$$i_t = \frac{nFAC^0 D^{1/2}}{\pi^{1/2} t^{1/2}}$$

The area of the glassy-carbon electrode was determined to be 0.084 cm² by using a diffusion coefficient of 0.629×10^{-5} cm²/s for potassium ferrocyanide in 2 M KCl solution.¹⁹

Results and Discussion

Previous studies demonstrate that the interaction of simple Lewis acids with $Fe(phen)_2(CN)_2$, $CpFe(CO)_2CN$, or $Cp_4Fe_4(CO)_4$ produces significant shifts in $\nu(CN)$ and $\nu(CO)$.^{1,10,11} In addition, the color of $Fe(phen)_2(CN)_2$ solutions changes dramatically upon introduction of Lewis acids and the associated shifts in electronic spectra are well documented.¹ These spectral fingerprints were employed in the present research to characterize the metal complex species in the molten salt medium as the acidity of the melt was changed.

The equilibrium shown in eq 1 links the three principal anionic species present in the room temperature aluminum chloride/*n*-butylpyridinium chloride molten salt melts.²⁰ Previous workers have



considered this melt as an acid–base system in which an acid is defined as a Cl^- acceptor and a base is defined as a Cl^- donor. For this reason, systems with a $AlCl_3$ to butylpyridinium chloride ratio, M_R , less than 1.0 are commonly referred to as “basic” whereas, for $M_R > 1$, the melt is referred to as “acidic”.²⁰ In the present report, some basic electroactive organometallic compounds are shown to form adducts with chloride-rich melts having M_R less than 1. Therefore, we refer to these melts as less acidic rather than basic.

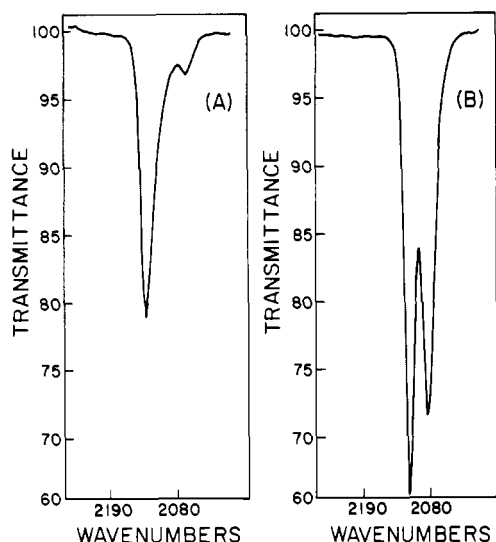
- (2) Shriver, D. F.; Alich, A. *Inorg. Chem.* **1972**, *11*, 2984.
- (3) (a) Wang, H.-K.; Choi, H. W.; Muetterties, E. L. *Inorg. Chem.* **1981**, *20*, 2661. (b) Choi, H. W.; Muetterties, E. L. *Ibid.* **1981**, *20*, 2664.
- (4) Collman, J. P.; Finke, R. G.; Cawse, J. N.; Brauman, J. I. *J. Am. Chem. Soc.* **1978**, *100*, 4766.
- (5) Horwitz, C. P.; Shriver, D. F. *Adv. Organomet. Chem.* **1984**, *23*, 219.
- (6) Robinson, J.; Osteryoung, R. A. *J. Am. Chem. Soc.* **1979**, *101*, 323.
- (7) (a) Schilt, A. A. *J. Am. Chem. Soc.* **1960**, *82*, 3000. (b) Schilt, A. A. *Inorg. Chem.* **1964**, *3*, 1323.
- (8) Hamer, N. K.; Orgel, L. E. *Nature (London)* **1961**, *190*, 439.
- (9) (a) King, R. B. *Inorg. Chem.* **1966**, *5*, 2227. (b) White, A. J.; Cunningham, A. J. *J. Chem. Educ.* **1980**, *57*, 317.
- (10) Kristoff, J. S.; Shriver, D. F. *Inorg. Chem.* **1973**, *12*, 1788.
- (11) Kristoff, J. S.; Shriver, D. F. *Inorg. Chem.* **1974**, *13*, 499.
- (12) Robinson, J.; Osteryoung, R. A. *J. Am. Chem. Soc.* **1980**, *102*, 4415.
- (13) Cheek, G. T.; Osteryoung, R. A. *J. Electrochem. Soc.* **1982**, *29*, 2488.
- (14) Sahami, S.; Osteryoung, R. A. *Electrochim. Acta* **1985**, *30*, 143.
- (15) (a) Gale, R. J.; Motyl, K. M.; Job, R. *Inorg. Chem.* **1983**, *22*, 130. (b) Chum, H. L.; Koran, D.; Osteryoung, R. A. *Inorg. Chem.* **1981**, *20*, 3304.
- (16) Perrin, D. D.; Armarego, W. L. F.; Perrin, D. R. *Purification of Laboratory Chemicals*; Pergamon: New York, 1980.
- (17) Shriver, D. F. *The Manipulation of Air Sensitive Compounds*; McGraw-Hill: New York, 1969; p 96.

- (18) Cottrell, F. G. Z. *Phys. Chem., Stoichiom. Verwandtschaftsl.* **1902**, *42*, 385.
- (19) Adams, R. N. *Electrochemistry at Solid Electrodes*; Marcel Dekker: New York, 1969.
- (20) (a) Lipsztajn, M.; Osteryoung, R. A. *J. Electrochem. Soc.* **1985**, *132*, 1126. (b) Karpinski, Z. J.; Osteryoung, R. A. *Inorg. Chem.* **1984**, *23*, 1491. (c) Lipsztajn, M.; Osteryoung, R. A. *J. Electrochem. Soc.* **1983**, *130*, 1968.

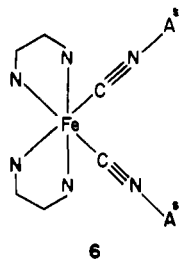
Table I. Spectral Data and Half-Wave Potentials for Fe(phen)₂(CN)₂

solvent or M_R^a	$\nu(\text{CN}), \text{cm}^{-1}$	$\lambda, ^b \text{nm}$	$E_{1/2}, ^c \text{V}$
0.75	2135 vs, 2072 w	505 sh, 472 [7200]	>0.7
0.90	2135 vs, 2073 w	502 sh, 460 [6900]	>0.8
1.00	2136 vs, 2112 sh, 2075 w	500 sh, 433 [6200], 392 sh	>1.0
1.25	2116 vs, 2087 vs	428 sh, 391 [4900]	1.33
1.50	2116 vs, 2086 vs	420 sh, 390 [4700]	1.31
2.00	2112 vs, 2080 vs	410 sh, 376 [4400]	1.47
CH ₂ Cl ₂	2083 vs	603 [9900], 540 sh, 370 [2300]	0.53 ^d
Nujol	2079, 2066		

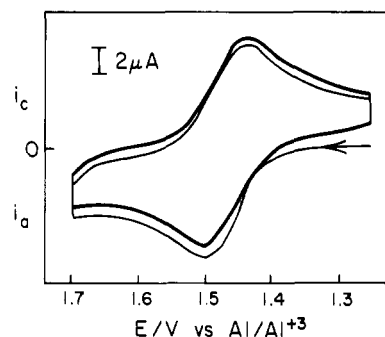
^a $M_R = \text{AlCl}_3:n\text{-butylpyridinium chloride}$. ^b Molar extinction coefficients ($\text{M}^{-1} \text{cm}^{-1}$) are enclosed in brackets. ^c Values are relative to Al/Al^{3+} in $M_R = 2.0$ melt. ^d This value was recorded vs. Ag wire and has been adjusted to correspond to the Al/Al^{3+} couple in the $M_R = 2.0$ melt reference.

**Figure 1.** Infrared spectra of Fe(phen)₂(CN)₂: (A) less acidic melt, $M_R = 0.85$; (B) strong acid melt, $M_R = 2.0$.

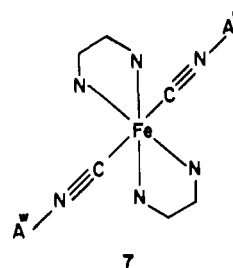
Fe(phen)₂(CN)₂ (1). In the less acidic electrolyte, $M_R = 0.75$, this iron cyanide complex forms a deep red solution with the major absorption maximum at 472 nm, and in the strongly acidic electrolyte, $M_R = 2.0$, the color is bright yellow ($\lambda_{\text{max}} = 376 \text{ nm}$). These bands are blue-shifted from the maximum for Fe(phen)₂(CN)₂ in CH₂Cl₂ solution ($\lambda_{\text{max}} = 603 \text{ nm}$), indicating that, in both instances, a Lewis acid is attached to the nitrogen end of the cyanide ligands. The bright yellow solution observed for the complex in the $M_R = 2.0$ melt has an electronic spectrum that is blue-shifted by 30 nm from the spectrum of Fe(phen)₂(CNBBR₃)₂ and is nearly identical with that of [Fe(phen)₂(CNH)₂]²⁺, which exists in 12 M H₂SO₄.^{1,8} Therefore, the species present in the $M_R = 2.0$ melt must result from coordination by a strong Lewis acid, A^s, with an acceptor strength greater than BBr₃. As shown in Table I, the CN stretches for the complex in this melt occur at 2112 (vs) and 2080 (vs) cm⁻¹ (Figure 1), which is reasonable for the *cis*-diadduct **6**.⁸ By contrast, the IR



spectrum for the complex in the less acidic melt $M_R = 0.75$ (Figure 1) exhibits a very strong absorption maximum at 2135 cm⁻¹ and

**Figure 2.** Cyclic voltammogram of Fe(phen)₂(CN)₂ in the strong acid melt, $M_R = 2.0$ (scan rate = 200 mV/s).

a very weak absorption band at 2072 cm⁻¹. The single strong band suggests a *trans* structure with acceptor groups attached to both CN ligands.⁸ Judging from the moderate blue shift in the visible spectrum, the acceptor strength of this weak Lewis acid, A^w, is significantly lower than the Lewis acid designated as A^s in **6**.²¹ The adduct formed when $M_R < 1.0$ is indicated in **7**.



Closer inspection of the $\nu(\text{CN})$ bands observed for **1** reveals that, in melts of all acidities, the band width at half-height, $w_{1/2}$, is $22 \pm 2 \text{ cm}^{-1}$. Therefore, the single peak observed for **7** could contain two $\nu(\text{CN})$ bands with a separation, $\Delta\nu(\text{CN})$, of $22 \pm 2 \text{ cm}^{-1}$ or less as would be expected for a *cis* arrangement of the CN-A^w ligands (cf. **6**, $\Delta\nu(\text{CN}) = 32 \text{ cm}^{-1}$, and the trend toward smaller $\Delta\nu(\text{CN})$ with decreasing acceptor ability of A reported for Fe(phen)₂(CN-A^s)₂).¹ However, the large shift in $\nu(\text{CN})$ observed for **7** relative to **1** indicates that the difference between **6** and **7** does not arise solely from the difference in acceptor strength of A^s and A^w. For this reason, formulation of the adducts as *cis*-Fe(phen)₂(CN-A^s)₂ for **6** and *trans*-Fe(phen)₂(CN-A^w)₂ for **7** seems logical.

In previous work both molecular orbital calculations and empirical observations were used to establish a direct correlation between the oxidation potential of Fe(phen)₂(CN-A)₂ and the acceptor ability of A. For A = BX₃ (X = F, Cl, Br), the Fe^{2+/3+} couple was reported to shift by 0.60, 0.66, and 0.69 V, respectively, relative to the parent complex.¹ In the present study, dissolution of Fe(phen)₂(CN)₂ in melts with $M_R > 1.0$ resulted in shifts of 0.78–0.94 V (Table I), indicating that the acceptor strength of A^s is greater than the acceptor strength of the boron trihalides. A representative cyclic voltammogram of Fe(phen)₂(CN)₂ in the $M_R = 2.0$ melt is shown in Figure 2. The Fe^{2+/3+} couple of Fe(phen)₂(CN)₂ was not observable in melts with $M_R < 1$ because of the less positive anodic limit attainable in these melts.²⁰ Bulk electrolysis of Fe(phen)₂(CN)₂ in the $M_R = 1.5$ melt at 140 mV positive of the anodic wave consumed 0.95 faraday/mol of Fe(phen)₂(CN)₂ and produced a green solution characteristic of the

(21) The presence of traces of water in melts with $M_R < 1$ has been shown to result in the formation of HCl and aluminum-hydroxy species.²⁰ Therefore, the possibility was explored that protons might be responsible for the apparent acidity of these melts. To test this possibility, increasing amounts of water were added to the $M_R = 0.75$ melt and the growth of a broad IR band at 3300 cm⁻¹ was monitored. From these experiments the limit of detection for water is estimated to be 50 mM. IR spectra recorded on 10–200 mM solutions of Fe(phen)₂(CN)₂ in the $M_R = 0.75$ melt show no changes attributable to protonated species. Therefore, we conclude that the apparent acidity of the $M_R = 0.75$ melt does not arise from protons.

Table II. Spectral Data and Half-Wave Potentials for $\text{Cp}_4\text{Fe}_4(\text{CO})_4$

solvent or M_R^a	$\nu(\text{CO})$, cm^{-1}	$\lambda, ^b \text{nm}$	$E_{1/2}(\text{Fe}_4^{0/+})^c$, V
0.75	1634	765 [1800], 660 [1300], 394 [17 000]	0.28
0.90	1634	765 [1800], 660 [1300], 394 [17 000]	0.28
1.0	1634	760 [1800], 660 [1400], 394 [15 000]	0.26
1.5	1458	657 [8200], 382 [24 000], 337 [35 000]	0.26
2.0	1458	654 [5600], 382 [16 000], 340 [23 000]	0.27
CH_2Cl_2	1638	770 [2100], 660 [1500], 394 [18 000], 280 sh	0.25
CH_3CN^d	1623	775 [3500], 645 [2500], 390 [18 000], 280 sh	0.19 ^e

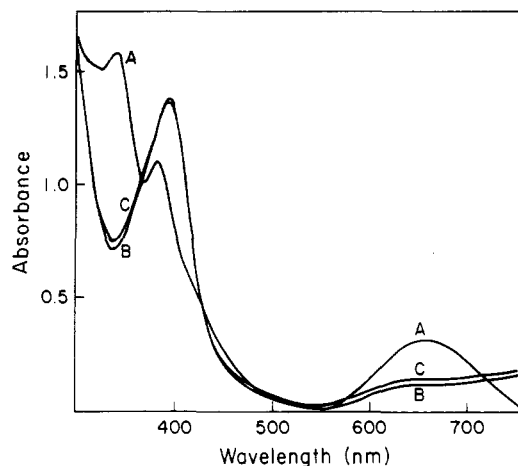
^a $M_R = \text{AlCl}_3:n$ -butylpyridinium chloride. ^b Molar extinction coefficients are enclosed in brackets. ^c Values are relative to Al/Al^{3+} in $M_R = 2.0$ melt. ^d Reference 23. ^e $E_{1/2}$ adjusted to correspond to the Al/Al^{3+} couple in the $M_R = 2.0$ melt reference. ^f This value was recorded vs. Ag wire and has been adjusted to correspond to the Al/Al^{3+} couple in the $M_R = 2.0$ melt reference.

cationic species $[\text{Fe}(\text{phen})_2(\text{CN}-\text{A})_2]^+$.

$\text{Cp}_4\text{Fe}_4(\text{CO})_4$ (**2**). The structural, electrochemical, and spectroscopic properties of $\text{Cp}_4\text{Fe}_4(\text{CO})_4$ have been described in great detail.^{22,23} This tetranuclear cluster contains four face-bridging carbonyl ligands, all of which are susceptible to Lewis acid attack. In fact, mono-tetrakis(aluminum tribromide) adducts have been formed and characterized by IR spectroscopy.¹¹ This cluster was chosen for study in the molten salts because it is extremely robust in solution.²³ The infrared spectrum of $\text{Cp}_4\text{Fe}_4(\text{CO})_4$ dissolved in CH_2Cl_2 exhibits a single carbonyl absorption at 1640 cm^{-1} .¹¹ The mono-tetraadducts of this compound with AlBr_3 exhibit very characteristic spectra. A large decrease in $\nu(\text{CO})$ is observed for the carbonyl complexed to the acid, and a small increase in $\nu(\text{CO})$ is observed for the remaining uncomplexed carbonyl ligands.¹¹ In the less acidic melts, a single band is observed for this compound at 1634 cm^{-1} , indicating no interaction between cluster and melt (Table II). However, in melts with $M_R > 1.0$, the $\nu(\text{CO})$ band at 1634 cm^{-1} has been replaced by a new band at ca. 1458 cm^{-1} , indicating the formation of $\text{Cp}_4\text{Fe}_4(\text{CO}-\text{A}^*)_4$. An interesting effect was observed when the IR spectrum of $\text{Cp}_4\text{Fe}_4(\text{CO})_4$ was recorded immediately after dissolution in a melt with $M_R = 1.10$. Weak bands ($\omega_{1/2} = 30 \text{ cm}^{-1}$) appeared at ca. 1745 and 1428 cm^{-1} . After several hours the spectrum was retaken and revealed a single band at 1458 cm^{-1} . The appearance of the first two bands in this intermediate melt suggests the presence of $\text{Cp}_4\text{Fe}_4(\text{CO})(\text{CO}-\text{A}^*)_3$ (cf. $\text{Cp}_4\text{Fe}_4(\text{CO})(\text{COAlBr}_3)_3$: $\nu(\text{CO}) = 1755$ vs. 1470 sh, 1439 vs. cm^{-1}).¹¹ After several hours, however, the triadduct appears to cleanly convert to the tetraadduct as evidenced by the single $\nu(\text{CO})$ band (cf. $\text{Cp}_4\text{Fe}_4(\text{COAlBr}_3)_4$: $\nu(\text{CO}) = 1473 \text{ cm}^{-1}$).¹¹

The $\nu(\text{CO})$ bands between 1400 and 1700 cm^{-1} were difficult to observe because of intense aromatic C-C stretching and deformation bands arising from the *n*-butylpyridinium cation.²⁴ In the weakly acidic melts the single CO stretch at 1634 cm^{-1} was observable only when a 0.015-mm spacer was used in the IR cell, and even under these conditions the data must be viewed with caution. However, our interpretation of the IR data is substantiated by the UV-vis data presented below.

The UV-vis spectrum of $\text{Cp}_4\text{Fe}_4(\text{CO})_4$ dissolved in weakly acidic melts is identical with the spectrum observed for this complex in CH_2Cl_2 (Figure 3) and so provides additional proof that no interaction occurs between the cluster and the weakly acidic melts. Unlike the continuous blue shift observed for $\text{Fe}(\text{phen})_2(\text{CN})_2$ in melts of increasing acidity, no shift in peak position is observed until the point where $M_R = 1.0$ is passed. As

**Figure 3.** Electronic spectra of $\text{Cp}_4\text{Fe}_4(\text{CO})_4$: (A) strong acid melt, $M_R = 2.0$; (B) less acidic melt, $M_R = 0.75$; (C) CH_2Cl_2 .**Table III.** CO and CN Stretching Frequencies (cm^{-1}) for $\text{CpFe}(\text{CO})_2\text{CN}^a$

solvent or M_R^b	$\nu(\text{CN})$	$\nu(\text{CO})_{\text{sym}}$	$\nu(\text{CO})_{\text{asym}}$	$\Delta\nu(\text{CO})_{\text{asym}}$
0.75, 0.90	2120	2055	2010	0
1.5	2140	2065	2030	20
2.0	2140	2078	2040	30
CH_2Cl_2	2120	2055	2010	

^a Frequencies are accurate to $\pm 5 \text{ cm}^{-1}$. ^b $M_R = \text{AlCl}_3:n$ -butylpyridinium chloride.

shown in Figure 3 and Table II, the spectrum changes drastically when the melt is made strongly acidic and then remains unchanged as the acidity is increased. These results are consistent with the IR results and indicate that when $M_R < 1$, no $\text{Cp}_4\text{Fe}_4(\text{CO})_4$ -melt interaction occurs whereas adduct formation does occur when $M_R > 1$.

The electrochemical experiments in the molten salts show no shift in the potential of the $[\text{Cp}_4\text{Fe}_4(\text{CO})_4]^{0/+}$ couple over the entire acidity range. The other two couples, $[\text{Cp}_4\text{Fe}_4(\text{CO})_4]^{0/-}$ and $[\text{Cp}_4\text{Fe}_4(\text{CO})_4]^{+/2+}$ are not accessible in the molten salts because of the narrow potential window.²⁰ Bulk electrolysis of $\text{Cp}_4\text{Fe}_4(\text{CO})_4$ in the $M_R = 1.5$ melt at 150 mV positive of the anodic wave consumed 1.0 faraday/mol of $\text{Cp}_4\text{Fe}_4(\text{CO})_4$. The insensitivity of the first oxidation potential to O coordination in the strongly acidic melt indicates that the HOMO of **2** does not contain a significant contribution from $\sigma\text{-M-CO}$ and $\pi\text{-M-CO}$ interactions. This interpretation is consistent with extended Hückle calculations for $\text{Cp}_4\text{Fe}_4(\text{CO})_4$, which show that the highest occupied orbitals are mainly localized on M and are insensitive to M-CO interactions.²⁵ The sensitivity of the UV-vis spectrum of $\text{Cp}_4\text{Fe}_4(\text{CO})_4$ to acidity indicates that the excited state must contain considerable contributions from $\sigma\text{-MCO}$ and/or $\pi\text{-MCO}$ orbitals. This interpretation agrees with the observation that the CO stretching frequency is much lower for $[\text{Cp}_4\text{Fe}_4(\text{CO})_4]^-$ (where the LUMO is occupied) than for $\text{Cp}_4\text{Fe}_4(\text{CO})_4$.²³

Since the $\text{Cp}_4\text{Fe}_4(\text{CO})_4$ cluster might be bonded to the melt through extended $\text{M}_3\text{CO-AlCl}_3\text{-Cl-AlCl}_3\cdots$ interactions it was of interest to determine the magnitude of the diffusion coefficients, D , for $\text{Cp}_4\text{Fe}_4(\text{CO})_4$ dissolved in various melts. In melts with $M_R = 0.75, 0.90,$ and 1.5 at 40°C , values of D were determined to be $0.28 \times 10^{-7}, 0.85 \times 10^{-7},$ and $1.5 \times 10^{-7} \text{ cm}^2/\text{s}$ respectively. These results imply that coordination of the cluster to the strongly acidic melts (as evidenced by the IR study described above) has little effect on its mobility. The values of D obtained for $\text{Cp}_4\text{Fe}_4(\text{CO})_4$ are approximately 1 order of magnitude lower than those values reported Cp_2Fe ,²⁶ which indicates that the cluster

(22) Neuman, M. A.; Trinh-Toan; Dahl, L. F. *J. Am. Chem. Soc.* **1972**, *94*, 3383.

(23) Ferguson, J. A.; Meyer, T. J. *J. Am. Chem. Soc.* **1972**, *94*, 3409.

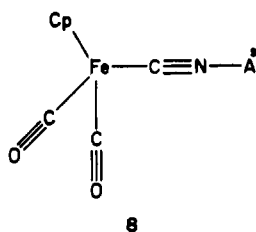
(24) Tait, S.; Osteryoung, R. A. *Inorg. Chem.* **1984**, *23*, 4352.

(25) (a) Bottomley, F.; Grein, F. *Inorg. Chem.* **1982**, *21*, 4170. (b) Trinh-Toan; Fehlhhammer, W. P.; Dahl, L. F. *J. Am. Chem. Soc.* **1972**, *94*, 3389.

(26) Karpinski, Z. J.; Nanjundiah, C.; Osteryoung, R. A. *Inorg. Chem.* **1984**, *23*, 3358.

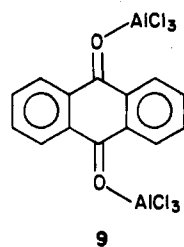
is less mobile than the monomer. This difference in mobility was also observed in CH₂Cl₂ containing 0.50 M TBABF₄ where values of *D* for Cp₄Fe₄(CO)₄ and Cp₂Fe were found to be 2.3 × 10⁻⁵ and 8.0 × 10⁻⁵ cm²/s, respectively. Since the diffusion coefficient for the cluster is surprisingly close to that of Cp₂Fe, we conclude that either the cluster interacts with discrete species contained in the melt or that if it does coordinate to extended aluminum chloride chains, then these adducts are highly labile.

CpFe(CO)₂(CN) (3). The infrared spectrum of this complex dissolved in the less acidic melts is identical with the spectrum obtained in CH₂Cl₂ (Table III) indicating a lack of adduct formation. In strongly acidic melts, however, large shifts to higher energy occur for ν(CN), ν(CO)_{sym} and ν(CO)_{asym}, and the intensity of the CN stretch increases greatly. These changes are indicative of adduct formation through the CN ligand of the complex. The large shift implies that the acidic species must have a very high electron-pair acceptor strength. Therefore we formulate the adduct formed in these melts as **8**.

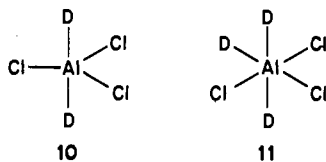


A previous study from this group described the use of CpFe(CO)₂(CN) as a convenient and reliable guide to trends in the electron pair acceptor strength of acids.¹⁰ The relative strength of the group III (group 13³²) trihalides was inferred to be BF₃ < BCl₃ < BBr₃ and AlCl₃ < GaCl₃ < BCl₃ from shifts in ν(CO)_{asym}, which occurred upon coordination of the acid to the cyanide ligand.¹⁰ The data in Table III show that the Al species in the weakly acidic melts are of lower acceptor strength than all of the group III trihalides. Additionally, the strongly acidic melts contain species much higher in acceptor strength than the group III trihalides. These results are in agreement with the results obtained for Fe(phen)₂(CN)₂ and Cp₄Fe₄(CO)₄ and further stress the very wide range of acidity available in this molten salt system.

Nature of A^s and A^w. The structures of the adducts formed in the molten salt are not clear because AlCl₃ is known to interact in many different ways with donors. Several inorganic and organic carbonyl compounds are known to form 1:1 adducts of type **9** with



AlCl₃.^{27,28} With donor solvents such as HNMe₂, THF, dioxane, and morpholine the formation of 2:1 adducts, **10**, is favored²⁹ and with pyridine a 3:1 adduct, **11**, has been isolated.³⁰ In sterically



- (27) Butts, S. B.; Holt, E. M.; Strauss, S. H.; Alcock, N. W.; Stimson, R. E.; Shriver, D. F. *J. Am. Chem. Soc.* **1979**, *101*, 5864.
 (28) Giallonardo, R.; Susz, B. P. *Helv. Chim. Acta* **1971**, *54*, 2402.
 (29) (a) Muller, G.; Kruger, C. *Acta Crystallogr., Sect. C: Cryst. Struct. Commun.* **1984**, *C40*, 628. (b) Boardman, A.; Small, R. W. H.; Worrall, I. J. *Acta Crystallogr., Sect. C: Cryst. Struct. Commun.* **1983**, *39*, 433. (c) Cowley, A. H.; Cushner, M. C.; Davis, R. E.; Riley, P. E. *Inorg. Chem.* **1981**, *20*, 1179. (d) Ahmed, A.; Schwarz, W.; Weidlein, J.; Hess, H. *Z. Anorg. Allg. Chem.* **1977**, *434*, 207.

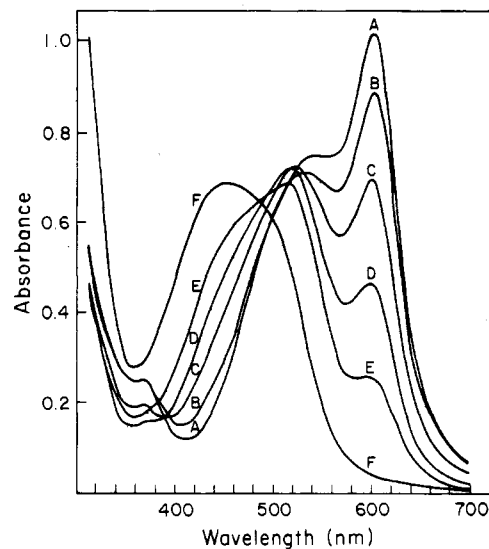
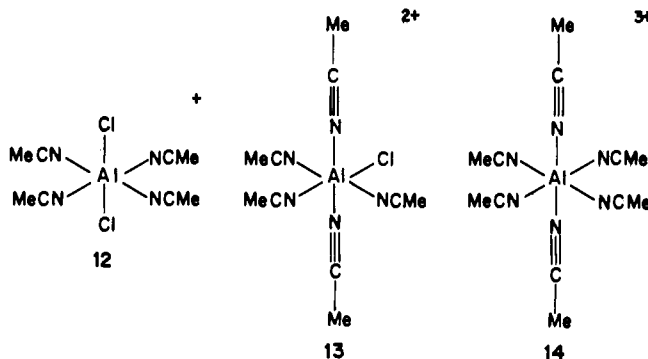


Figure 4. Electronic spectra of Fe(phen)₂(CN)₂ in (A) CHCl₃ and in CHCl₃ with added amounts of AlCl₃: (B) 0.5 equiv; (C) 1.0 equiv; (D) 2.0 equiv; (E) 5.0 equiv; (F) 15 equiv.

unencumbered coordinating solvents, such as CH₃CN, Cl⁻ is displaced from AlCl₃, resulting in the cationic complexes **12–14**.³¹



The studies described here do not clearly identify A^s and A^w. However, since Al₂Cl₇⁻ is the predominant species in the strongly acidic melts and AlCl₄⁻ is present in the less acidic melts, it seems likely that A^s is a dimeric form of A^w. The UV-vis spectrum of **1** in CHCl₃ undergoes a blue shift when increasing amounts of AlCl₃ are added (Figure 4), which is similar to the shift observed on increasing *M_R*. Therefore, we might formulate A^w as AlCl₃ on the basis of this study and a study in which adduct **9** was isolated from a melt with *M_R* = 1.2.¹³ This interpretation would suggest that A^s is Al₂Cl₆. The spectroscopic data support this formulation by indicating that A^s is a stronger acceptor than BCl₃ while A^w is a weaker acceptor. Previous spectroscopic studies have shown that AlCl₃ is a weaker electron pair acceptor than BCl₃.¹⁰

Conclusions

An extremely wide range of Lewis acidity can be achieved by varying the ratio of AlCl₃ to *n*-butylpyridinium chloride contained in the molten salt mixture. All of the organometallics formed complexes with Lewis acid species in melts with AlCl₃:BPC > 1. In melts with AlCl₃:BPC < 1 a Lewis acid interaction was

- (30) Pullman, P.; Hensen, K.; Bats, J. W. *Z. Naturforsch., B: Anorg. Chem., Org. Chem.* **1982**, *37*, 1312.
 (31) (a) Beattie, I. R.; Jones, P. J.; Howard, J. A. K.; Smart, L. E.; Gilmore, C. J.; Akitt, J. W. *J. Chem. Soc., Dalton Trans* **1979**, 528. (b) Jones, D. E. H.; Wood, J. L. *J. Chem. Soc. A* **1971**, 3135.
 (32) The periodic group notation in parentheses is in accord with recent actions by IUPAC and ACS nomenclature committees. A and B notation is eliminated because of wide confusion. Groups IA and IIA become groups 1 and 2. The d-transition elements comprise groups 3 through 12, and the p-block elements comprise groups 13 through 18. (Note that the former Roman number designation is preserved in the last digit of the new numbering: e.g., III → 3 and 13.)

observed only for the most basic compound, $\text{Fe}(\text{phen})_2(\text{CN})_2$. The three organometallic compounds studied were shown to exhibit high stability in melts of all compositions. For $\text{Fe}(\text{phen})_2(\text{CN})_2$ dissolved in the strongly acidic melts, the position of the +2/+3 couple was shown to shift by ca. 0.80 V, indicating that electron density is strongly drawn away from the metal center. However, for $\text{Cp}_4\text{Fe}_4(\text{CO})_4$, the potential of the 0/+ couple remains fixed over the entire range of acidity. This is in keeping with MO calculations, which show that the HOMO of $\text{Cp}_4\text{Fe}_4(\text{CO})_4$ is localized on the metal framework. This versatile room-temper-

ature molten salt system is an excellent medium for studying the influence of Lewis acids on the redox reactions of organometallics.

Acknowledgment. We thank the Gas Research Institute (Grant 5082-260-0693) for financial support and Energy Research and Generation, Inc., for supplying the reticulated vitreous carbon. C.W. gratefully acknowledges helpful comments from Professors R. A. Osteryoung and John Wilkes concerning the nature of molten salts and from Dr. John G. Gaudiello concerning electrochemical techniques.

Contribution from the Department of Chemistry,
University of Iowa, Iowa City, Iowa 52242

Synthesis and Magnetic Resonance Spectroscopy of Novel Phenolato-Bridged Manganese(III) and Iron(III)-Manganese(III) Porphyrin Complexes

Gregory M. Godziela, David Tilotta, and Harold M. Goff*

Received June 24, 1985

A novel manganese(III) porphyrin dimeric compound and an Fe(III)-Mn(III) heterodinuclear complex have been synthesized and structurally characterized by electronic and magnetic resonance spectroscopy. Metal derivatives of 5-(2-hydroxyphenyl)-10,15,20-tritolyloporphyrin are susceptible to dimerization through formation of phenolato bridges. Monomeric (phenolato)-manganese(III) porphyrin complexes have also been prepared for the first time. Proton NMR spectral comparisons between the manganese(III) dimeric species and simple (phenolato)manganese(III) tetraphenylporphyrin provide justification for the phenolato-bridge hypothesis, allow for complete assignment of the porphyrin dimer NMR signals, and also permit comparison of spin-delocalization patterns for iron(III) and manganese(III) compounds. A spin-only magnetic moment of $5.0 \mu_B$ and linear Curie law proton NMR plots indicate minimal antiferromagnetic coupling between the two manganese(III) centers of the dimeric species. The Fe(III)-Mn(III) heterodinuclear complex has been prepared in situ, but attempts to isolate the species free of homo dimers have been unsuccessful. Proton NMR and electron spin resonance spectra of solutions containing the mixed-metal dimer show new signals that are not seen in the spectra of the parent iron(III) and manganese(III) dimeric species.

Introduction

The coordination chemistry of manganese porphyrins is less well developed than that of corresponding biologically relevant iron porphyrins. More efficient porphyrin-manganese ion orbital overlap appears to weaken the interaction of axial ligands for the manganese center.¹ In comparison with iron(III) porphyrin analogues, manganese(III) porphyrins show lower affinity for addition of two axial ligands. Formation of the low-spin d^4 complex requires addition of two very strong field ligands such as imidazolate^{2,3} or cyanide ions.^{3,4} In noncoordinating organic solvents manganese(III) porphyrins are most likely to exist as neutral five-coordinate species bearing an anionic axial ligand. Coordinating solvents readily displace the anionic ligand to yield solvate complexes.

As is the case for other strong-field chelated manganese coordination compounds, the +3 oxidation state represents the air-stable form. Reduction to the +2 state⁵ and oxidation to higher oxidation states are possible. Oxidation may be either porphyrin-centered⁶ or metal-centered,⁷ depending on the nature of the axial ligand(s). Synthetic manganese porphyrins have recently been shown to exhibit properties as oxidative catalysts that rival

those of the iron analogues.⁸ It thus appears important to improve our understanding of fundamental manganese porphyrin chemistry and to increase the diversity of available manganese porphyrin compounds.

Among manganese(III) porphyrins there are few examples of well-defined dimeric complexes. Polymeric imidazolato-bridged species have been characterized in the solid state.² The μ -oxo or μ -hydroxo dimer resulting from base hydrolysis⁹ remains structurally undefined, although the further oxidized μ -oxo manganese(III)-manganese(IV) and manganese(IV)-manganese(IV) derivatives are unambiguously identified.⁷ By comparison, numerous dimeric iron(III) porphyrin systems are known.

A dimeric iron(III) tetraarylporphyrin complex bridged by phenolato residues of the porphyrin has recently been prepared and structurally characterized both in solution and in the solid state.¹⁰ The manganese(III) analogue is described here. This represents the first well-defined soluble dimeric manganese(III) porphyrin complex. In addition, it is shown that a novel mixed manganese(III)-iron(III) derivative is readily generated. Preparation of other mixed-metal complexes with the general structure I should also be possible.

Experimental Section

Manganese Porphyrin Synthesis. The functionalized 5-(2-hydroxyphenyl)-10,15,20-tritolyloporphyrin (TTOHPH₂) was prepared by condensation of 3 equiv of *p*-tolylaldehyde, 1 equiv of salicylaldehyde, and 4 equiv of pyrrole in a propionic acid reflux. The desired porphyrin was conveniently separated from other porphyrin products by sequential chromatography on alumina and silica gel columns.^{10,11}

- (1) Boucher, L. J. *Coord. Chem. Rev.* **1972**, *7*, 289-329.
- (2) Landrum, J. T.; Hatano, K.; Scheidt, W. R.; Reed, C. A. *J. Am. Chem. Soc.* **1980**, *102*, 6729-6735.
- (3) Hansen, A. P.; Goff, H. M. *Inorg. Chem.* **1984**, *23*, 4519-4525.
- (4) Scheidt, W. R.; Lee, Y. J.; Luangdilok, W.; Haller, K. J.; Anzai, K.; Hatano, K. *Inorg. Chem.* **1983**, *22*, 1516-1522.
- (5) Kadish, K. M.; Kelly, S. *Inorg. Chem.* **1979**, *18*, 2968-2971.
- (6) Goff, H. M.; Phillippi, M. A.; Boersma, A. D.; Hansen, A. P. *Adv. Chem. Ser.* **1982**, *No. 201*, 357-376.
- (7) (a) Schardt, B. C.; Hollander, F. J.; Hill, C. L. *J. Am. Chem. Soc.* **1982**, *104*, 3964-3972. (b) Smegal, J. A.; Hill, C. L. *Ibid.* **1983**, *105*, 2920-2922. (c) Smegal, J. A.; Schardt, B. C.; Hill, C. L. *Ibid.* **1983**, *105*, 3510-3515. (d) Camenzind, M. J.; Hollander, F. J.; Hill, C. L. *Inorg. Chem.* **1983**, *22*, 3776-3784.

- (8) Smegal, J. A.; Hill, C. L. *J. Am. Chem. Soc.* **1983**, *105*, 3515-3521 and references therein.
- (9) Fleischer, E. B.; Palmer, J. M.; Srivastava, T. S.; Chatterjee, A. *J. Am. Chem. Soc.* **1971**, *93*, 3162-3167.
- (10) Goff, H. M.; Shimomura, E. T.; Lee, Y. J.; Scheidt, W. R. *Inorg. Chem.* **1984**, *23*, 315-321.